



Published in final edited form as:

*Bone*. 2018 January ; 106: 90–95. doi:10.1016/j.bone.2015.03.021.

## Comparison of cyclic and impact-based reference point indentation measurements in human cadaveric tibia

Lamya Karim<sup>a,b,c,\*</sup>, Miranda Van Vliet<sup>a</sup>, Mary L. Bouxsein<sup>a,b</sup>

<sup>a</sup>Center for Advanced Orthopedic Studies, Beth Israel Deaconess Medical Center, 330 Brookline Avenue, Boston, MA 02215, United States

<sup>b</sup>Department of Orthopedic Surgery, Harvard Medical School, 330 Brookline Avenue, Boston, MA 02215, United States

<sup>c</sup>Department of Bioengineering, University of Massachusetts Dartmouth, 285 Old Westport Road, Dartmouth, MA 02747, USA

### Abstract

Although low bone mineral density (BMD) is strongly associated with increased fracture risk, up to 50% of those who suffer fractures are not detected as high-risk patients by BMD testing. Thus, new approaches may improve identification of those at increased risk for fracture by in vivo assessment of altered bone tissue properties, which may contribute to skeletal fragility. Recently developed reference point indentation (RPI) allows for assessment of cortical bone indentation properties in vivo using devices that apply cyclic loading or impact loading, but there is little information available to assist with interpretation of RPI measurements. Our goal was to use human cadaveric tibia to determine: 1) the associations between RPI variables, cortical bone density, and morphology; 2) the association between variables obtained from RPI systems using cyclic, slow loading versus a single impact load; and 3) age-related differences in RPI variables. We obtained 20 human tibia and femur pairs from female donors (53–97 years), measured total hip BMD using dual-energy X-ray absorptiometry, assessed tibial cortical microarchitecture using high-resolution peripheral quantitative computed tomography (HR-pQCT), and assessed cortical bone indentation properties at the mid-tibial diaphysis using both the cyclic and impact-based RPI systems (Biodent and Osteoprobe, respectively, Active Life Scientific, Santa Barbara, CA). We found a few weak associations between RPI variables, BMD, and cortical geometry; a few weak associations between measurements obtained by the two RPI systems; and no age-related differences in RPI variables. Our findings indicate that in cadaveric tibia from older women RPI measurements are largely independent of age, femoral BMD, and cortical geometry. Furthermore, measurements from the cyclic and impact loading RPI devices are weakly related to each other, indicating that each device reflects different aspects of cortical bone indentation properties.

\*Corresponding author at: Department of Bioengineering, University of Massachusetts Dartmouth, 285 Old Westport Road, Dartmouth, MA 02747, USA. Fax: +508 999 9139. lkarim@umassd.edu (L. Karim).

## Keywords

Aging; Bone; Indentation

---

## 1. Introduction

Skeletal fractures are associated with increased disability and mortality and are highly prevalent among the elderly. Although low bone mineral density (BMD) is strongly associated with increased fracture risk, there are many who suffer from fractures despite having normal bone density. Up to 50% of those who experience a fracture are not identified as having osteoporosis by BMD testing [1]. It has been proposed that there are several other factors that contribute to skeletal fragility including altered bone microarchitecture and changes in tissue-level mechanical properties. A few techniques are available for non-invasive assessment of bone morphology and microstructure, and several clinical studies have demonstrated the contribution of bone microarchitecture to bone strength and fracture risk assessment using these methods [2]. However, there is little *in vivo* information available on the contribution of altered bone matrix properties to skeletal fragility in humans because until recently the biomechanical properties of the bone tissue could not be assessed non-invasively. Prior studies have demonstrated altered bone matrix composition in those with a history of fracture, but required bone biopsies for analysis by Fourier transform infrared spectroscopy [3-6].

Recently developed reference point indentation (RPI) is a minimally-invasive technique that allows for assessment of cortical bone indentation properties via cyclic or impact based loading [7-10]. The bench-top Biodent system (Active Life Scientific, Santa Barbara, CA) measures the distance a test probe indents into bone using a specified load over multiple cycles, with a maximum load of 10 N (Fig. 1). Several variables, which are based on the force applied and indentation distance into the bone across one or all cycles, are calculated from these measurements [11]. Few data exist on this novel technique. One study by Gallant et al. combined indentation data collected from cyclic indentation of rat femurs, rat vertebrae, and dog ribs to demonstrate that indentation distance increase (increase in the indentation distance in the last cycle relative to that in the first cycle) is negatively correlated with apparent toughness estimated from whole bone biomechanical testing ( $r^2 = 0.51$ ) [12]. Two clinical studies using cyclic indentation of the mid-tibia demonstrated greater indentation distances in postmenopausal women with hip fractures compared to women without fractures [13,14].

In comparison, the hand-held Osteoprobe (Active Life Scientific, Santa Barbara, CA), designed for *in vivo* use in humans and large animals, measures the indentation distance following a single 30 N impact load (preceded by a 10 N preload, Fig. 2) [9]. A single variable, bone material strength index (BMSi), defined as the average indentation distance into bone due to the impact load normalized to the indentation distance measured on a polymethyl methacrylate (PMMA) reference phantom, is obtained from these measures. The Osteoprobe has been used to show that postmenopausal women with type 2 diabetes have approximately 10% lower BMSi than those without diabetes [15]. However, as emphasized

in a commentary by Jepsen and Schlecht [16], the two RPI systems have completely different loading profiles, and no studies have reported whether the variables acquired from these devices are comparable.

Moreover, there are limited data regarding the factors that may affect RPI measures and the age-related changes in RPI measures. For example, one study showed positive correlations between matrix mineralization measures assessed by Raman spectroscopy and indentation distances and energy dissipation assessed by RPI in diabetic rats [17], while contrastingly, another study indicated that tissue composition did not account for differences in RPI measures in a rat model of chronic kidney disease versus controls [18]. One investigation showed that indentation distances and energy dissipation assessed by RPI decrease with age in porcine bone [11], whereas another showed that indentation distances were greater in old human bone compared to young bone [19]. Altogether, there is limited information on what factors influence RPI measurements in human bone, and how these properties change with age.

Hence, the goals of this study were to use human cadaveric tibias to determine: 1) the associations between RPI measurements and cortical bone density and morphology; 2) the association between indentation properties measured by the two systems and the inter-correlations between the multiple parameters derived from the cyclic indentation testing; and 3) age-related differences in RPI measurements. We hypothesized that indentation properties will be associated with cortical tissue mineral density and morphology, that cyclic and impact-based RPI measurements will be correlated with each other, and that RPI measurements will worsen with age.

## 2. Methods

### 2.1. Specimen collection

We obtained 20 human tibia and femur pairs from female donors with an age range of 53 to 97 years (average:  $74.2 \pm 14.6$  years) (Anatomic Gifts Registry, Hanover, MD). Specimens were harvested fresh and frozen at  $-20^{\circ}\text{C}$  until testing. None of the donors had any history of diabetes, bone metabolic disorders, or bisphosphonate use.

### 2.2. Bone mineral density and geometry assessment

Total hip bone mineral density (BMD,  $\text{g}/\text{cm}^2$ ) was measured using dual-energy X-ray absorptiometry (DXA, QDR Discovery, Hologic Inc., Bedford, MA). During the scanning procedure, femurs were submerged in a water bath and fixed in a position similar to that used during in vivo DXA scans. We measured cortical tissue mineral density (Ct.TMD,  $\text{mg}/\text{cm}^3$ ), cortical thickness (Ct.Th, mm), and cortical porosity (Ct.Po, %) at the mid-tibia using high-resolution peripheral quantitative computed tomography (HR-pQCT, XtremeCT, Scanco Medical AG, Bassersdorf, Switzerland). Briefly, 110 slices were obtained at  $82\ \mu\text{m}$  nominal resolution (X-ray tube current 95 mA, effective energy 60 kVp). The scan region was centered at the site of RPI measurements at the midshaft, defined as the exact midpoint between proximal and distal ends of the bone.

### 2.3. Reference point indentation

Tibias were thawed overnight, kept hydrated with saline, and indented at the mid-diaphysis using both cyclic and impact loading devices (Active Life Scientific, Santa Barbara, CA). Indentations were made within a  $\sim 0.25 \text{ cm}^2$  region to minimize site-based variation. For the cyclic loading device (Biodent), five separate indentation tests were performed 1 mm apart on the antero-medial surface of the tibia at 10 N maximum force, 2 Hz, for 20 cycles, and results from the five separate tests were averaged, following a protocol similar to other studies [13,14]. Indentations were made using a probe assembly consisting of a beveled reference probe with blunted end ( $\sim 5 \text{ mm}$  cannula length) and test probewith spherical tip ( $2.5 \mu\text{m}$  radius point) that tapers from a  $90^\circ$  cone shape to cylindrical shaft (BP2 probe, Active Life Scientific, Santa Barbara, CA). The following variables were measured (Fig. 1): indentation distance (ID, indentation distance measured in the first cycle [ $\mu\text{m}$ ]), creep indentation distance (CID, total indentation distance during the hold step of the first cycle [ $\mu\text{m}$ ]), average creep indentation distance (avg CID [ $\mu\text{m}$ ]), total indentation distance (TID, total indentation distance across all cycles [ $\mu\text{m}$ ]), indentation distance increase (IDI, increase in the indentation distance in the last cycle relative to that in the first cycle [ $\mu\text{m}$ ]), average energy dissipation (avg ED, area enclosed by the test's hysteresis loop from the third to last cycle [ $\mu\text{J}$ ]), unloading slope (US, unloading slope of the first cycle [ $\text{N}/\mu\text{m}$ ]), average unloading slope (avg US, average unloading slope from third to last cycle [ $\text{N}/\mu\text{m}$ ]), and average loading slope (avg LS, average loading slope from third to last cycle [ $\text{N}/\mu\text{m}$ ]). With the impact loading device (Osteoprobe), a minimum of eight separate indentation tests were performed 1 mm apart. More than 8 indentations were taken in the event that the Osteoprobe slipped or was not held perpendicular to the bone surface, and these instances were identified and confirmed by both the user and an accompanying assistant while conducting the measurements. These incorrectly obtained indentation measurements were discarded immediately during data collection and were not included in any analyses. An additional indentation measurement was taken in this case so that eight reliable data points were acquired. The indents were made on the antero-medial surface, while ensuring that previously tested regions were avoided. Each set of bone indentations was followed by five measurements on a PMMA reference phantom. BMSi was calculated as the average indentation distance into the bone normalized to the indentation distance into the PMMA reference phantom \* 100.

### 2.4. Statistical analyses

We tested whether the data were normally distributed using Shapiro-Wilk W tests. Indentation distances, avg. ED, and Ct.Po were not normally distributed, whereas age, loading and unloading slopes, BMSi, total hip BMD, Ct.TMD, and Ct.Th were normally distributed. Thus, non-parametric Spearman correlations ( $r_s$ ) were used to determine associations between cyclic and impact-derived variables, and also between all RPI variables, BMD, geometry, and age. Pearson correlations ( $r_p$ ) were used in cases in which both variables being compared were normally distributed (e.g. avg. US vs. avg. LS). Partial correlation analyses were conducted to confirm the relationships observed between RPI variables, Ct.TMD, Ct.Po, and Ct.Th while controlling for age. Differences between variables assessed in middle aged (53–69 years,  $n = 8$ ) and old aged (70–97 years,  $n = 12$ )

tibias were determined using unpaired Students *t*-test in the case of normally distributed variables and Mann-Whitney *U* tests in the case of variables with nonnormal distribution.

### 3. Results

Descriptive data for DXA, HR-pQCT, Biodent, and Osteoprobe variables are reported in Table 1. The mean age of the donors was  $74.9 \pm 14.6$  years (range: 53–97 years).

RPI variables from cyclic indentation were variably correlated with each other (Table 2), with relationships ranging from weak to very strong. For example, ID in the first cycle of loading was very strongly correlated with TID ( $r^2 = 0.96$ ). In comparison, IDI was moderately correlated to TID ( $r^2 = 0.37$ ) and energy dissipation ( $r^2 = 0.28$ ), but unrelated to unloading slope measurements. Because of strong interrelationships between several variables (e.g. ID vs. TID, CID vs. avg. CID, US vs. avg. US, avg. US vs. avg. LS), we selected one from each pair of these variables to assess relationships with BMSi, age, and bone morphology (Figs. 3 and 4). Some cyclic indentation variables showed a trend to be weakly correlated with BMSi (Fig. 3), but none reached significance. Specifically, BMSi was negatively correlated to TID ( $r_s = -0.36$ ,  $p = 0.12$ ), US ( $r_p = -0.44$ ,  $p = 0.053$ ), and avg. US ( $r_p = -0.41$ ,  $p = 0.08$ ), but was not associated with any of the other variables.

RPI measures were either unrelated or weakly related to cortical density, porosity, and thickness at the tibial midshaft (Fig. 4). For example, BMSi was moderately positively correlated with cortical TMD ( $r_p = 0.44$ ,  $p = 0.055$ ) and moderately negatively associated with porosity ( $r_s = -0.37$ ,  $p = 0.08$ ), but was independent of cortical thickness. None of the cyclically-derived indentation measurements were related to cortical TMD, porosity, or thickness. Partial correlation analyses indicated that after controlling for age, BMSi still had a trend of a positive correlation with cortical TMD ( $r^2 = 16\%$ ,  $p = 0.09$ ), but was independent of cortical porosity and thickness. Additionally, IDI was shown to be negatively correlated with cortical TMD ( $r^2 = 18\%$ ,  $p = 0.06$ ) and positively with porosity ( $r^2 = 42\%$ ,  $p < 0.05$ ), while average energy dissipation was positively correlated with porosity ( $r^2 = 25\%$ ,  $p < 0.05$ ). Total hip BMD was not related to any cyclically-derived variables, but was moderately negatively related to BMSi ( $r = -0.39$ ,  $p = 0.09$ ).

There were no age-related differences in cyclic indentation variables or BMSi. RPI variables were similar in the middle-age (53–69 years) and older (70–97 years) specimens even though cortical thickness was lower ( $-13.6\%$ ,  $p < 0.05$ ) and cortical porosity higher ( $+125.1\%$ ,  $p < 0.05$ ) in the older group.

### 4. Discussion

In this study, we investigated the associations between RPI variables, cortical bone density, and morphology; the association between variables obtained by both two RPI methodologies and age-related differences in RPI variables. In contrast to our hypotheses, we found that: 1) BMSi was independent of cortical thickness and weakly correlated with total hip BMD, cortical TMD, and porosity, while cyclically-derived indentation variables were not correlated to femoral BMD or tibial cortical morphology; 2) measurements made with the

two RPI systems were either unrelated or very weakly related to each other; and 3) indentation measures were not associated with age.

The first goal of this study was to determine the associations between RPI measurements and hip BMD, cortical bone density and morphology. We initially found that BMSi was weakly to moderately positively correlated with total hip BMD and tibial cortical tissue mineral density, and weakly negatively correlated with tibial cortical porosity. Thus, it is implied that less mineralized bone tends to have less resistance to indentation which allows for larger indentation distances. However, partial correlation analyses showed that the relationship with TMD and porosity became weaker or insignificant. Also while controlling for age, IDI was negatively correlated with cortical tissue mineral density, and both IDI and average energy dissipation were positively correlated with cortical porosity. However, these relationships were also weak and were driven by few data points. Because our results showed weak relationships between indentation variables and cortical porosity or thickness, it appears that microarchitecture does not have a major influence on indentation properties. Pilot studies conducted in our laboratory in a rat model also show that there are no relationships between cortical geometry and RPI variables, thus providing evidence that RPI variables reflect properties that are independent of bone morphology.

We also hypothesized that cyclic and impact-based RPI measurements would be correlated with each other. We found that impact-derived BMSi was unrelated or weakly related to indentation measures from cyclic loading. Importantly, in one instance (i.e., BMSi vs TID, Fig. 2), the correlation appears to be driven by a few data points with very high values of TID. These measurements with very high TID values were technically sound. Notably, however, these specimens were obtained from donors who were wheelchair bound, had a history of glucocorticoid use, or were noted in the donor history records as having “poor bone and muscle.” This suggests that inclusion of a greater variety of donors (e.g. wide age range, variety of health problems) might provide additional insight into relationships between cyclic and impact-derived indentation measurements. However, based on our results obtained from women in an age group at risk for fracture, the relationships between indentation measures derived from cyclic and impact loading are weak or nonexistent. These findings further emphasize that ex vivo studies conducted using the cyclic loading may not translate directly to altered indentation measurements acquired in vivo via the impact loading device. These two systems likely measure different aspects of bone material properties. The measurements derived from Biodent's cyclic loading profile may illustrate creep or fatigue associated crack growth in the bone tissue whereas the measurement derived from Osteoprobe's impact loading profile may reflect energy dissipation due to a major crack created by a single high-velocity, high-energy load.

Our final aim was to determine age-related differences in RPI variables. RPI variables were not worse with increasing age, nor did they differ between the middle- and older-aged groups, suggesting that these measures are not sensitive to age-related changes in human bone in this particular age group. To further clarify these findings, future work will need to assess tissue level mechanical properties in these specimens to understand whether RPI measures are truly independent of age in women over age 50 or whether there are minimal differences in RPI measures due to limited changes in mechanical properties in this

age group. Of note, a classic study by Burstein et al. illustrated that cortical bone specimens from human cadavers (21 to 86 years) showed a progressive deterioration in numerous mechanical properties (e.g. ultimate stress, ultimate strain, energy-to-fracture) with increased age in femurs and a deterioration in ultimate strain and energy-to-fracture with increased age in tibias [20]. These changes were evident even within the age group presented in our current study. Thus, it is possible that the RPI variables we measured did not differ with age in this age group despite known changes in tissue mechanical properties in human cadaveric bone.

There have been no previous studies that assessed age-related differences in BMSi in human bone, though Farr et al. reported lower BMSi values in postmenopausal women with longstanding type 2 diabetes [15]. One study using the indentation measurements from cyclic loading found that IDI, CID, TID, and average ED decreased with age while average US increased with age in porcine bone [11]. This study incorporated cortical bone ranging from 1 to 48 months in age, which encompasses the full growth and development stages as well as mature stages in a porcine model [21]. The current study used bones from women aged 53 to 97 years, but did not include any younger individuals. This may explain, in part, why we did not detect any age-related differences in indentation variables—either a larger sample is needed to detect subtle age-related differences that occur in an older population, and/or specimens from much younger individuals are needed to identify possible differences in RPI variables across bone acquisition/ growth, adulthood, and aging.

In conclusion, we determined that RPI variables are only weakly associated with bone mineral density, and are independent of cortical thickness and age. Moreover, the cyclically-derived and impact-derived indentation variables are weakly related to each other, indicating that they provide different information about cortical bone tissue properties. Thus, it is unlikely that patterns in ex vivo cyclic indentation measurements will be replicated directly by in vivo indentation measurements based on impact loading. Additional studies are needed to more fully define the utility of both cyclic- and indentation-based measurements for understanding skeletal fragility.

## Acknowledgements

We would like to thank Active Life Scientific for their technical support while conducting this study. Funding was provided by a grant from the Merck Investigator Studies Program and NIH T32AG023480 (Karim). The content is solely the responsibility of the authors and does not necessarily represent the official views of the NIH.

## References

- [1]. Schuit SCE, van der Klift M, Weel AEAM, de Laet CEDH, Burger H, Seeman E, Hofman A, Uitterlinden AG, van Leeuwen JPTM, Pols HAP, Fracture incidence and association with bone mineral density in elderly men and women: the Rotterdam Study, *Bone* 34 (2004) 195–202. [PubMed: 14751578]
- [2]. Cheung AM, Adachi JD, Hanley DA, Kendler DL, Davison KS, Josse R, Brown JP, Ste-Marie LG, Kremer R, Erlandson MC, Dian L, Burghardt AJ, Boyd SK, High-resolution peripheral quantitative computed tomography for the assessment of bone strength and structure: a review by the Canadian Bone Strength Working Group, *Curr. Osteoporos. Rep* 11 (2013) 136–146. [PubMed: 23525967]

- [3]. Gourion-Arsiquaud S, Faibish D, Myers E, Spevak L, Compston J, Hodsman A, Shane E, Recker RR, Boskey ER, Boskey AL, Use of FTIR spectroscopic imaging to identify parameters associated with fragility fracture, *J. Bone Miner. Res* 24 (2009) 1565–1571. [PubMed: 19419303]
- [4]. Donnelly E, Meredith DS, Nguyen JT, Gladnick BP, Rebolledo BJ, Shaffer AD, Lorich DG, Lane JM, Boskey AL, Reduced cortical bone compositional heterogeneity with bisphosphonate treatment in postmenopausal women with intertrochanteric and subtrochanteric fractures, *J. Bone Miner. Res* 27 (2012) 672–678. [PubMed: 22072397]
- [5]. Misof BM, Gamsjaeger S, Cohen A, Hofstetter B, Roschger P, Stein E, Nickolas TL, Rogers HF, Dempster D, Zhou H, Recker R, Lappe J, McMahon D, Paschalis EP, Fratzl P, Shane E, Klaushofer K, Bone material properties in premenopausal women with idiopathic osteoporosis, *J. Bone Miner. Res* 27 (2012) 2551–2561. [PubMed: 22777919]
- [6]. Malluche HH, Porter DS, Mawad H, Monier-Faugere MC, Pienkowski D, Low-energy fractures without low T-scores characteristic of osteoporosis: a possible bone matrix disorder, *J. Bone Joint Surg. Am* 95 (2013) e1391–6. [PubMed: 24088974]
- [7]. Hansma P, Yu H, Schultz D, Rodriguez A, Yurtsev EA, Orr J, Tang S, Miller J, Wallace J, Zok F, Li C, RS, Proctor A, Brimer D, Nogues-Solan X, Mellibovsky L, Pena MJ, Diez-Ferrer O, Mathews P, Randall C, Kuo A, Chen C, Peters M, Kohn D, Buckley J, Li X, Pruitt L, Diez-Perez A, Alliston T, Weaver V, Lotz J, The tissue diagnostic instrument, *Rev. Sci. Instrum* 80 (2009), 054303. [PubMed: 19485522]
- [8]. Randall C, Mathews P, Yurtsev E, Sahar N, Kohn D, Hansma PK, The bone diagnostic instrument III: testing mouse femora, *Rev. Sci. Instrum* 80 (2009) 065108. [PubMed: 19566227]
- [9]. Bridges D, Randall C, Hansma PK, A new device for performing reference point indentation without a reference probe, *Rev. Sci. Instrum* 83 (2012), 044301. [PubMed: 22559552]
- [10]. Hansma P, Turner P, Drake B, Yurtsev E, Proctor A, Mathews P, Lulejian J, Randall C, Adams J, Jungmann R, Garza-de-Leon F, Fantner G, Mkrtchyan H, Pontin M, Weaver A, Brown MB, Sahar N, Rossello R, Kohn D, The bone diagnostic instrument II: indentation distance increase, *Rev. Sci. Instrum* 79 (2008), 064303. [PubMed: 18601422]
- [11]. Rasoulian R, Raeisi Najafi A, Chittenden M, Jasiuk I, Reference point indentation study of age-related changes in porcine femoral cortical bone, *J. Biomech* 46 (2013) 1689–1696. [PubMed: 23676290]
- [12]. Gallant MA, Brown DM, Organ JM, Allen MR, Burr DB, Reference-point indentation correlates with bone toughness assessed using whole-bone traditional mechanical testing, *Bone* 53 (2013) 301–305. [PubMed: 23274349]
- [13]. Diez-Perez A, Guerri R, Nogues X, Caceres E, Pena MJ, Mellibovsky L, Randall C, Bridges D, Weaver JC, Proctor A, Brimer D, Koester KJ, Ritchie RO, Hansma PK, Microindentation for in vivo measurement of bone tissue mechanical properties in humans, *J. Bone Miner. Res* 25 (2010) 1877–1885. [PubMed: 20200991]
- [14]. Guerri-Fernandez RC, Nogues X, Quesada Gomez JM, Torres Del Pliego E, Puig L, Garcia-Giralt N, Yoskovitz G, Mellibovsky L, Hansma PK, Diez-Perez A, Microindentation for in vivo measurement of bone tissue material properties in atypical femoral fracture patients and controls, *J. Bone Miner. Res* 28 (2013) 162–168. [PubMed: 22887720]
- [15]. Farr JN, Drake MT, Amin S, Melton LJ III, McCready LK, Khosla S, In vivo assessment of bone quality in postmenopausal women with type 2 diabetes, *J. Bone Miner. Res* 29 (4) (2013) 787–795.
- [16]. Jepsen KJ, Schlecht SH, Biomechanical mechanisms: resolving the apparent conundrum of why individuals with type II diabetes show increased fracture incidence despite having normal BMD, *J. Bone Miner. Res* 29 (4) (2014) 784–786. [PubMed: 24496824]
- [17]. Hammond MA, Gallant MA, Burr DB, Wallace JM, Nanoscale changes in collagen are reflected in physical and mechanical properties of bone at the microscale in diabetic rats, *Bone* 60C (2013) 26–32.
- [18]. Newman CL, Moe SM, Chen NX, Hammond MA, Wallace JM, Nyman JS, Allen MR, Cortical bone mechanical properties are altered in an animal model of progressive chronic kidney disease, *PLoS One* 9 (2014), e99262. [PubMed: 24911162]



- [19]. Milovanovic P, Zimmermann EA, Riedel C, Scheidt AV, Herzog L, Krause M, Djonic D, Djuric M, Puschel K, Amling M, Ritchie RO, Busse B, Multi-level characterization of human femoral cortices and their underlying osteocyte network reveal trends in quality of young, aged, osteoporotic and antiresorptive-treated bone, *Biomaterials* 45 (2015) 46–55. [PubMed: 25662494]
- [20]. Burstein AH, Reilly DT, Martens M, Aging of bone tissue: mechanical properties, *J. Bone Joint Surg* 58 (1976) 82–86. [PubMed: 1249116]
- [21]. Feng L, Chittenden M, Schirer J, Dickinson M, Jasiuk I, Mechanical properties of porcine femoral cortical bone measured by nanoindentation, *J. Biomech* 45 (2012) 1775–1782. [PubMed: 22648144]

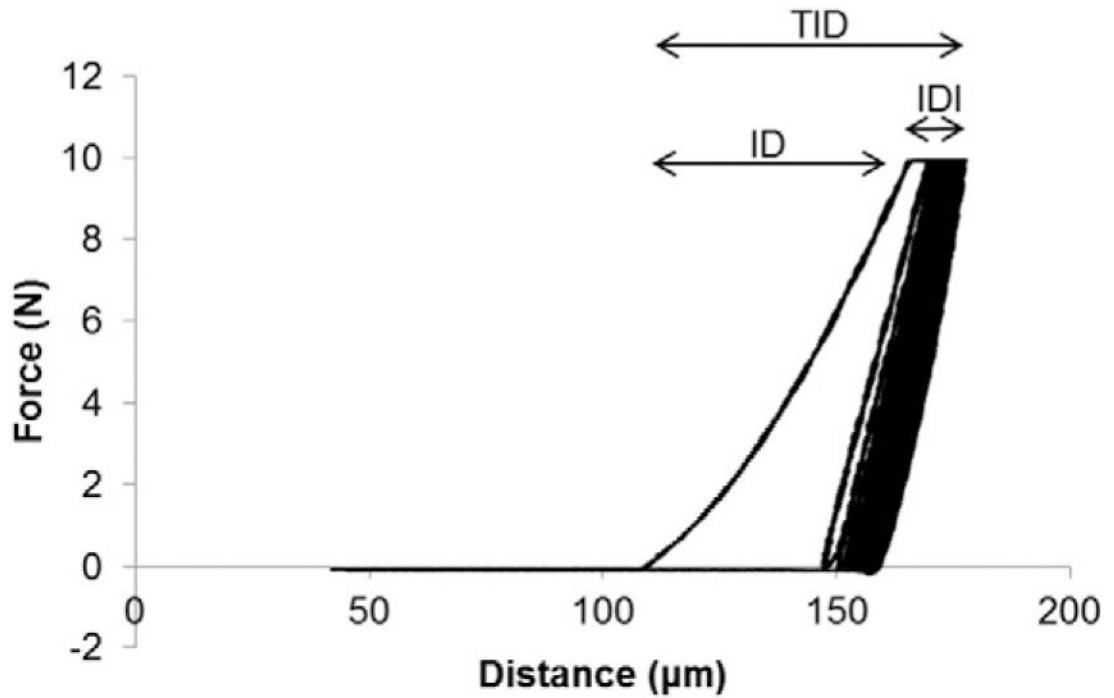


**Fig. 1.**

Force versus distance graph for a cyclic-based RPI test with 20 loading cycles. Variables derived from these curves include indentation distance (ID), total indentation distance (TID), indentation distance increase (IDI), loading and unloading slopes, and energy dissipation (ED). Average ED is calculated as the area within the test's hysteresis loop from the third to last cycle. The average slopes during loading and unloading are measured from the third to last cycle.

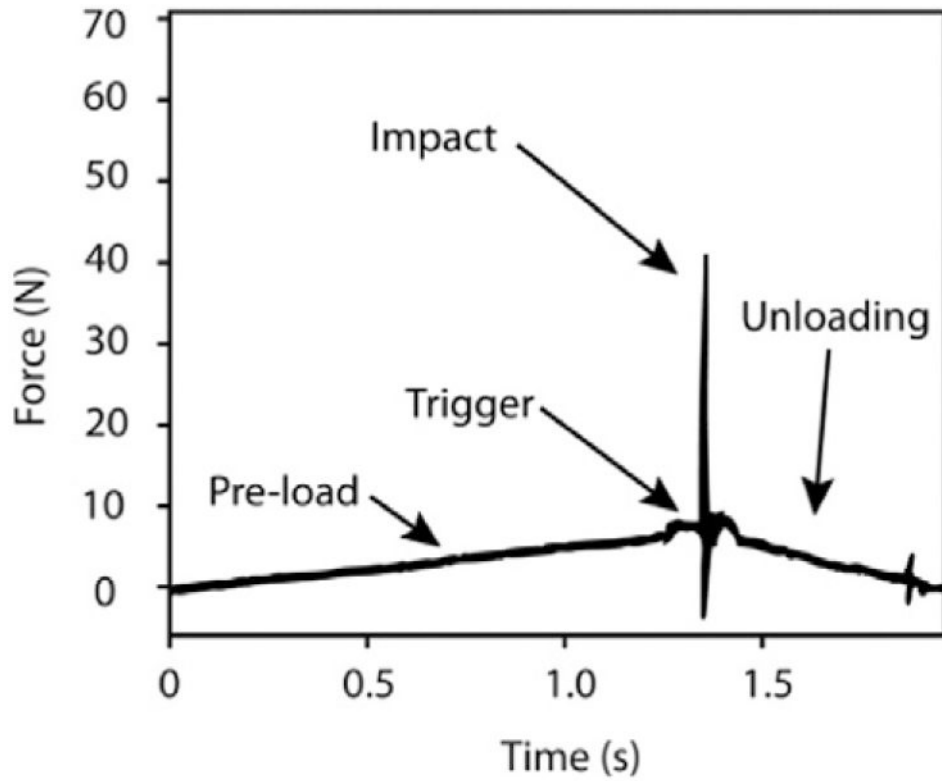


**Fig. 2.** Force versus time graph for an impact-based RPI test. Indentation distance is measured at the time of impact (on the order of 1 ms duration) from impact-based RPI tests and is normalized to the indentation distance into a PMMA reference phantom \* 100 to assess BMSi. Figure reprinted with permission from Bridges et al. [9].

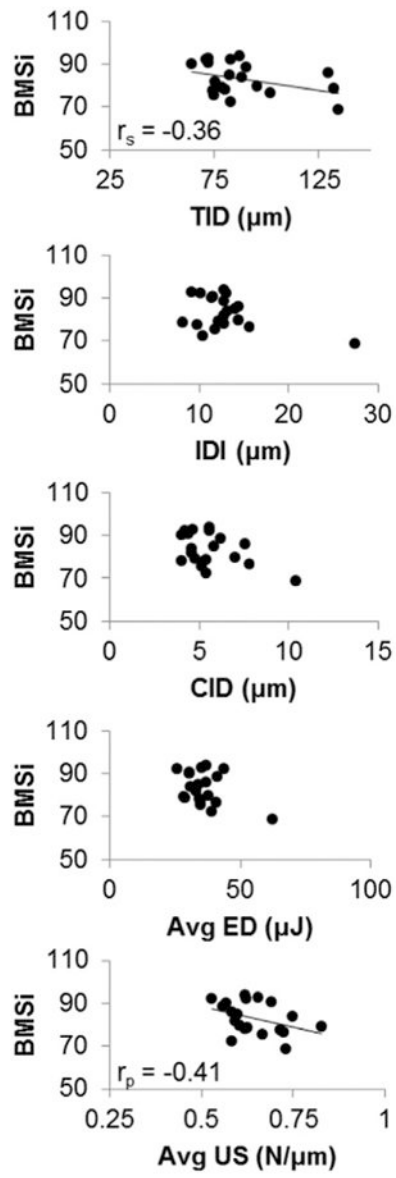


**Fig. 3.** Association between BMSi and cyclic indentation measurements.

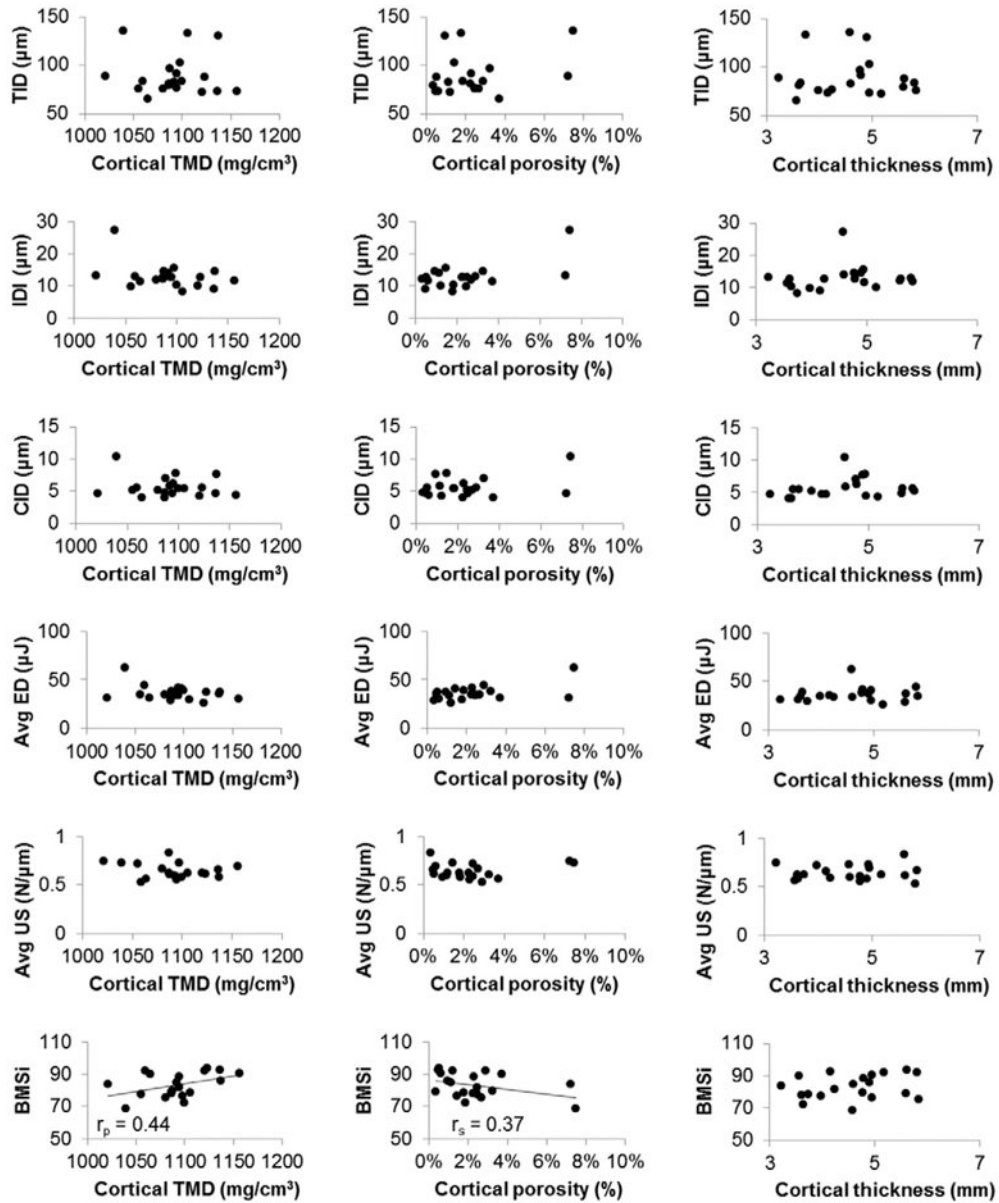


**Fig. 4.** Association between cortical tissue mineral density, porosity, and thickness at themid-tibia and indentation variables derived from cyclic and impact loading. Significant ( $p < 0.05$ ) or near significant relationships are shown with a regression line and correlation coefficient.

**Table 1**

Summary statistics of total hip BMD, tibial HR-pQCT measures, and RPI variables.

	Average $\pm$ standard deviation (range)
DXA	
Total hip BMD (g/cm <sup>2</sup> )	0.69 $\pm$ 0.15 (0.35–0.89)
HR-pQCT	
Ct.TMD (mg HA/cm <sup>3</sup> )	1092 $\pm$ 34(1021–1156)
Ct.Po (%)	2.34 $\pm$ 1.96 (0.33–7.46)
Ct.Th (mm)	4.59 $\pm$ 0.80 (3.22–5.83)
Cyclic loading (Biodent)	
ID ( $\mu$ m)	80.26 $\pm$ 20.01 (55.80–129.00)
CID ( $\mu$ m)	5.62 $\pm$ 1.57 (4.00–10.40)
Avg CID ( $\mu$ m)	1.54 $\pm$ 0.46 (1.00–2.80)
TID ( $\mu$ m)	88.61 $\pm$ 20.79 (64.20–134.60)
IDI ( $\mu$ m)	12.90 $\pm$ 3.89 (8.20–27.40)
US (N/ $\mu$ m)	0.60 $\pm$ 0.08 (0.50–0.78)
Avg US (N/ $\mu$ m)	0.64 $\pm$ 0.08 (0.53–0.83)
Avg LS (N/ $\mu$ m)	0.49 $\pm$ 0.05 (0.41–0.61)
Avg ED ( $\mu$ J)	36.05 $\pm$ 7.70 (26.06–62.34)
Impact loading (Osteoprobe)	
BMSi	83.06 $\pm$ 7.44 (68.44–93.63)

**Table 2**

Association<sup>‡</sup> between variables derived from cyclic indentation measurements.

	ID (µm)	CID (µm)	Avg CID (µm)	TID (µm)	IDI (µm)	US (N/µm)	Avg US (N/µm)	Avg LS (N/µm)	Avg ED (µJ)
ID (µm)	-	<b>+0.80<sup>**</sup></b>	<b>+0.69<sup>**</sup></b>	<b>+0.98<sup>**</sup></b>	<b>+0.52<sup>*</sup></b>	-0.05	+0.00	-0.14	<b>+0.53<sup>*</sup></b>
CID (µm)		-	<b>+0.86<sup>**</sup></b>	<b>+0.80<sup>**</sup></b>	<b>+0.61<sup>**</sup></b>	-0.14	-0.09	-0.31	<b>+0.75<sup>**</sup></b>
Avg CID (µm)			-	<b>+0.70<sup>**</sup></b>	<b>+0.48<sup>*</sup></b>	<b>-0.38<sup>x</sup></b>	-0.31	<b>-0.46<sup>*</sup></b>	<b>+0.86<sup>**</sup></b>
TID (µm)				-	<b>+0.61<sup>**</sup></b>	-0.04	+0.00	-0.19	<b>+0.55<sup>*</sup></b>
IDI (µm)					-	+0.03	-0.03	<b>-0.39<sup>x</sup></b>	<b>+0.53<sup>*</sup></b>
US (N/µm)						-	<b>+0.98<sup>**</sup></b>	<b>+0.73<sup>**</sup></b>	-0.30
Avg US (N/µm)							-	<b>+0.84<sup>**</sup></b>	-0.29
Avg LS (N/µm)								-	<b>-0.55<sup>*</sup></b>
Avg ED (µJ)									-

Pearson correlation coefficient ( $r_p$ ) shown in italics.

\* p 0.05.

\*\* p 0.01.

<sup>x</sup> 0.5 < p 0.10.

<sup>‡</sup> Spearman correlation coefficient ( $r_s$ ).